4D vs. 2D flow MRI in 109 patients with dilated ascending aorta: Improved Assessment of Peak Systolic Velocity

Martin Fasshauer[1,2], Alexander L. Powell[3], Alex J. Barker[3], Susanne Schnell[3], Joachim Lotz[1,2], and Michael Markl[3,4]

[1]*Institute for Diagnostic And Interventional Radiology, University Medical Center Goettingen, Goettingen, Lower saxony, Germany,* [2]*German Center for Cardiovascular Research, DZHK, partner site Goettingen, Germany,* [3]*Department of Radiology, Nortwestern University, Chicago, IL, United States,* [4]*Department of Biomedical Engineering, Northwestern University, Chicago, IL, United States*

Introduction: Thoracic aortic aneurysms (TAAs) have an annual incidence of around 10 cases/100,000 patient years [1] and are a life threatening disease. To date, the most common denominator for surgical intervention is based on measurements of aortic size, and more specifically, the diameter of the aneurysm. While easy to assess, a significant number of patients with TAAs still die from aortic rupture, the most devastating consequence of this aortic disease, before current guidelines recommend surgical intervention. The measurement of aortic diameter alone thus seems to be an insufficient predictor for risk of rupture. In this study, we applied 4D flow MRI for the in-vivo assessment of aortic 3D blood flow in the entire thoracic aorta in a total of 109 patients with either aortic aneurysm or dilated aorta. The aim was to expand our understanding of the impact of TAA on aortic hemodynamics beyond the standard analysis based on single measurements in 2D planes.

Methods: Our cohort consisted out of 109 patients (23 females) undergoing standard-of-care cardiac MRI at 1.5T or 3T MR systems (Siemens, Germany) for monitoring of aortic dimensions. Imaging included ECG gated time-resolved (CINE) cardiac MRI for the evaluation of cardiac function and SV as well as contrast enhanced MR angiography for the quantification of aortic dimensions. In addition, 2D CINE PC-MRI with single-direction through-plane velocity encoding was acquired. Blood flow was measured below the aortic valve, in-plane with the valve and above. For the assessment of aortic hemodynamics, time-resolved 3D phase-contrast MRI with three-directional velocity encoding (4D flow MRI) was acquired during free breathing using respiratory and prospective ECG gating covering the entire thoracic aorta in an oblique sagittal orientation as described previously [2]. Pulse sequence parameters were as follows: flip angle = 15°, TE = 2.2-2.9, TR = 4.6-5.4ms, spatial resolution = 2.1-3.4mm x 2.1-2.5mm x 2.2-3.0mm, temporal resolution = 36.8-43.2ms, total acquisition time was on the order of 8-15 minutes. Patients were diagnosed with aneurysm (n=47) of the ascending aorta (AAo) if the diameter in the middle AAo (MAA) or at the sinus of Valsalva (SOV) was greater than 4.5 cm (Figure 1). 4D flow analysis included manual placement of analysis planes above the valve. The plane location was individually adjusted to coincide with peak systolic velocity that was visually identified using a color-coded velocity map. In addition, analysis planes below the valve were adjusted to avoid measurements of subvalvular complex flow patterns interfering with accurate retrograde flow measurement. Net flow measurements in all planes were compared with calculated stroke volume (SV) from functional cine imaging. Peak velocity was directly compared with the radiologist report for peak velocity values, while regurgitation fraction was calculated by dividing retrograde flow below the valve by the forward flow measured above the valve (analogue to the method used in 2D PC-MRI). Complex flow patterns were visually assessed and graded as follows: Grade 0 – no complex flow patterns, Grade 1 - complex flow patterns usually observed in healthy controls (such as forward helical flow), Grade 2 – deflection of AAo mainstream from the aortic wall with subsequent complex flow patterns in forward direction (for example vortex), Grade 3 – same as 2 but with minimized forward flow, Grade 4 – multiple vortices and helices without apparent flow direction.

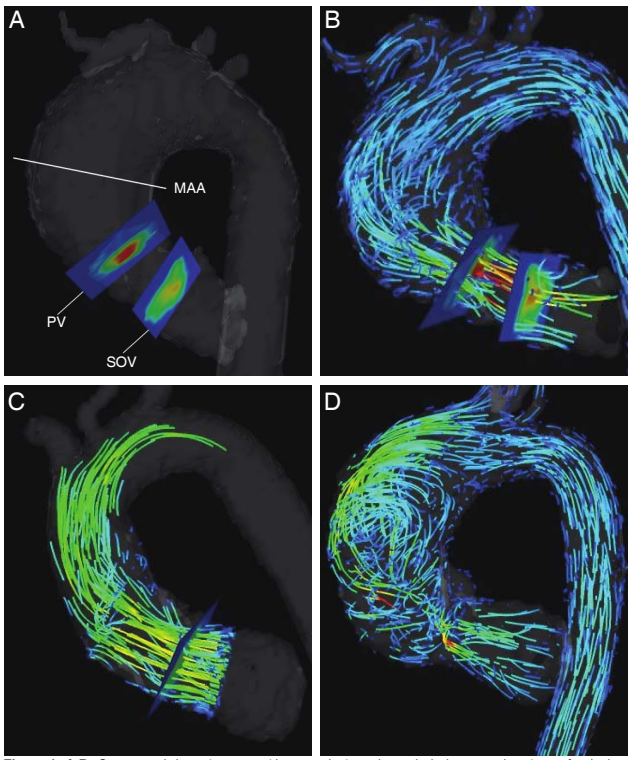

Figure 1. A,B: Segmented thoracic aorta with two velocity color-coded planes at the sinus of valsalva (SOV) and visually assessed peak velocity (PV) via 4D pathlines (B). Example of planes for measurement of aortic diameters at the middle ascending aorta (MAA) and SOV . **C:** Particle tracing from the aortic valve with grade 1 flow and some deflection of the blood flow from the aortic wall. **D:** Particle tracing of the aortic volume with grade 3 flow with multiple vortices and visually reduced forward flow in the aortic arch and descending aorta

	Cine	2D PC-MRI	4D PC-MRI		
Table 1b	**short axis stack**		**visual peak velocity**	**aortic valve**	**below aortic valve**
Peak velocity in m/s		1.9 ± 1.0	2.1** ± 1.0	1.9 ± 0.9	0.7** ± 1.5
Stroke volume in ml/beat	93 ± 24		99 ± 28	95 ± 32	87 ± 23

Table 1b	**Controls with aneurysm (n=21)**	**Controls without aneurysm (n=24)**	**Mild AI with aneurysm (n=18)**	**Moderate or severe AI with aneurysm (n=8)**	**Moderate or severe AI without aneurysm (n=20)**	**Any kind of AS without aneurysm (n=18)**
Visual peak velocity in 4D PC-MRI in m/s	1.5 ± 0.5	1.7* ± 0.6	1.5** ± 0.3	1.6 ± 0.3	2.4 ± 0.2	3.7 ± 1.0
Peak velocity in 2D PC-MRI in m/s	1.4 ± 0.6	1.4 ± 0.6	1.2 ± 0.3	1.7 ± 1.2	2.1 ± 0.2	3.4 ± 0.9

Table 1a: Comparison of peak velocity and stroke volume (mean ± SD) among all patients (n=109 for velocity and n=103 for SV). **1b:** Comparison of peak velocity among various subgroups as described in shown table. Statistic analysis was performed using repeated measurement one-way ANOVA with Tukey's multiple comparison test for peak velocity and beat volume. (*p < 0.05, **p<0.01, Prism 6.0f, Graphpad, La Jolla, CA, USA).

Results: 4D flow guided peak velocity measurement resulted in significantly higher values compared to reported 2D peak velocities, while peak velocity at the aortic valve was comparable to 2D PC-MRI. Due to the large number of patients with aortic insufficiency, peak velocity measured below the aortic valve was often negative, as a result of possible regurgitant jets in early diastole. Further analysis of 2D vs. 4D PC-MRI peak velocities using the Bland-Altman method comparison showed a mean bias of 0.22 m/s (95% limits of agreement +1.7 and -1.2). Mean bias for patients with or without aneurysm were comparably higher (0.28 m/s without aneurysms vs 0.14 m/s with aneurysms, limits of agreement +2.0; -1.5 and +1.1; -0.8 respectively). After exclusion of patients with aortic stenosis (n=18, AS), bias was 14.4% ± 3.2. Overall, SV did not significantly differ from SV derived from standard CINE MRI. The mean value of the complex flow pattern grading was 2.5 ± 1.1 (SD), showing a significant disagreement with a theoretical grading of 1 seen in control groups without aortic ectasia or aortic valve pathologies (Wilcoxon signed rank test, $p<0.0001$).

Discussion: 4D PC-MRI and 3D reconstruction of the TAA allowed for the fine tuning of flow analysis planes. Our findings indicate the potential of 4D flow MRI to better identify the optimal region for peak velocity quantification compared to standard 2D PC MR. Especially in dilated AAo's blood flow has been shown to be more complex than commonly seen in healthy volunteers. This is important because patients with complex flow will often not have the peak velocity vector lining up orthogonal to the 2D through-plane encode direction. Thus, there is a very high likelihood with through-plane encoding that the peak velocity is higher than that measured. 4D flow will capture all directions, in a volume, thus the peak velocity appears to better reconciled with the technique. This finding is in accordance to previously published studies comparing 4D to 2D PC-MRI in patients with aortic stenosis [3]. In addition, SV could reliably be assessed using 4D flow MRI as compared to the gold standard CINE MRI. Our study shows that 4D PC-MRI has the potential to yield more accurate peak velocities in complex flow environments, even in the absence of aortic stenosis.

Acknowledgements: Grant support: NIH grant K25HL119608; NIH grant R01HL115828, and Deutsche Forschungsgemeinschaft (DFG) Grant #HA 5399/3-1.

References: 1. Clouse, W.D., et al. JAMA, 1998. **280**(22): p. 1926-9. **2.** Markl, M., et al. J Magn Reson Imaging, 2007. **25**(4): p. 824-31. **3.** Nordmeyer, S., et al. J Magn Reson Imaging, 2013. **37**(1): p. 208-16.